Pediatr Radiol (2010) 40:1476–1484
DOI 10.1007/s00247-010-1709-4

ORIGINAL ARTICLE

Assessment of retromesenteric position of the third portion of the duodenum: an US feasibility study in 33 newborns

David K. Yousefzadeh · Lisa Kang · Laura Tessicini

Received: 2 October 2009 / Revised: 29 April 2010 / Accepted: 5 May 2010 / Published online: 16 June 2010

Abstract
Background US can be used to assess bowel and does not require ionizing radiation or the administration of contrast material. Prior studies of the duodenum with US are limited.
Objective This study assesses the success rate of US demonstration of the third portion of the duodenum (D3) between the superior mesenteric artery (SMA) and the aorta in newborns to exclude malrotation based on embryologic and anatomic principles.
Material and methods Thirty-three newborns underwent US studies. The structures between the SMA and the aorta, including D3, were evaluated in axial and longitudinal planes. The length of time to acquire diagnostic images was recorded.
Results In both the axial and longitudinal planes, D3 was seen between the SMA and the aorta in all 33 infants, including some with abundant bowel gas. The mean length of time to acquire diagnostic images was 34 s.
Conclusion Bedside US successfully illustrated the retromesenteric position of D3 in all 33 infants. Overlying gas-filled bowel was effectively effaced by graded compression. The short study duration indicates the practicality of the method. Further studies in broader patient populations and in correlation with other imaging and/or surgical findings is required to validate our technique.

Keywords Malrotation · Midgut volvulus · US · Duodenum · Embryology · Anatomy

D. K. Yousefzadeh (✉) · L. Kang · L. Tessicini
Department of Radiology, Comer Children's Hospital,
The University of Chicago,
5841 S. Maryland Ave., MC 2026,
Chicago, IL 60637, USA
e-mail: dyousefz@radiology.bsd.uchicago.edu

Introduction

Several imaging modalities have been used to diagnose or exclude malrotation and malrotation with volvulus [1–28]. The false-positive rate of upper gastrointestinal examination (UGI) has been reported to be as high as 15–30% [29, 30] and the false-negative rate up to 6% [29]. Many publications have addressed the shortcomings of UGI in the diagnosis and exclusion of malrotation [4–6, 8–10, 13].

The proponents of "evidence-based diagnosis" [29] and "the balance of evidence discipline" [30] have advocated a constellation of up to seven imaging studies, concluding that only collective knowledge from all these examinations can determine the correct diagnosis. Yet, if after exhausting all efforts, uncertainty continues, laparoscopic or surgical diagnosis might still have to be considered [30], an opinion echoed by a recent editorial [31].

The embryologic texts and the anatomic illustrations both indicate that in normal individuals D3 must be behind the SMA and in front of the aorta [32, 33]. Hence, to fulfill the embryologic and anatomic requirements, all it should take to unequivocally exclude malrotation and midgut volvulus is demonstrating D3 behind the SMA and in front of the aorta by cross-sectional imaging (Figs. 1 and 2), confirming that the gut has completed its embryologic journey and D3 is anatomically secured in the retroperitoneal compartment, immune from developing midgut volvulus. In malrotation D3 is always intraperitoneal [34] and anterior to the mesenteric vessels. Therefore, cross-sectional imaging, and in particular ultrasonography, is the most reliable and practical method to exclude malrotation because unlike UGI, US can prove that D3 is housed in the retromesenteric, retroperitoneal compartment [35].

Radiologists are quite familiar with the imaging features of the so-called SMA syndrome [36–39] in which D3 is

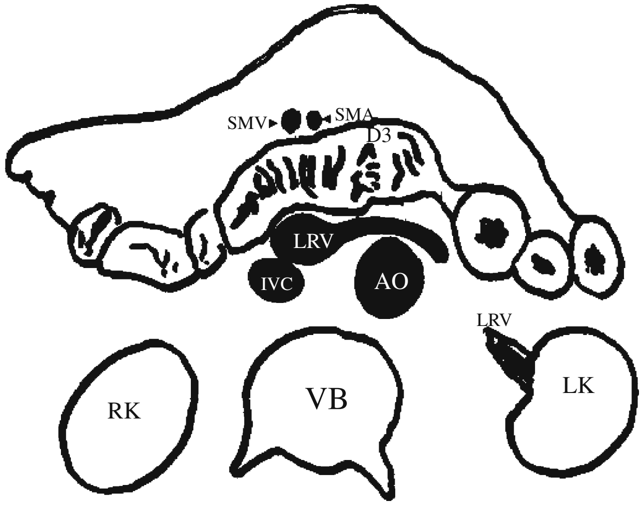

Fig. 1 Transverse anatomic sketch demonstrates the third portion of the duodenum (D3) between the SMA/SMV (*arrowheads*) and the aorta (*AO*). The left renal vein (*LRV*), inferior vena cava (*IVC*), left and right kidneys (*LK* and *RK*) and vertebral body (*VB*) are also shown

compressed between the aorta and the SMA. Therefore, our anatomically and embryologically based diagnostic method does not bear the shortcomings of UGI. Furthermore, the reliability of identification of a retromesenteric D3 in excluding malrotation has been mentioned in adult CT

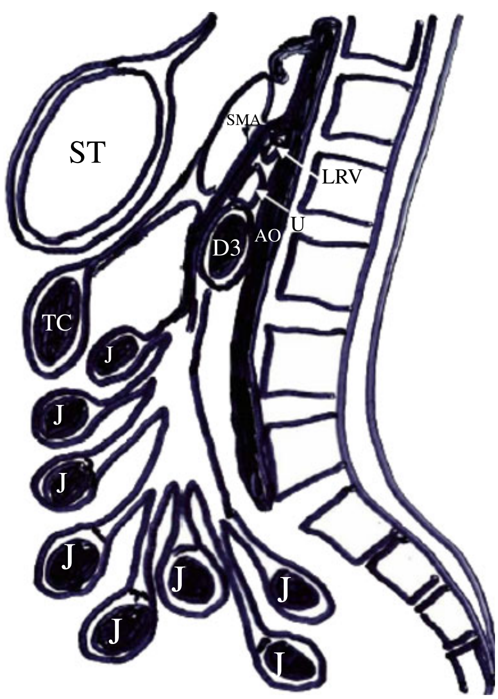

Fig. 2 Sagittal anatomic sketch shows the third portion of the duodenum (D3) between the SMA (*arrowhead*) and the aorta (*AO*). Two other retromesenteric structures, the left renal vein (*LRV*) and the uncinate process (*U*), are also shown. All the jejunal loops (*J*), the transverse colon (*TC*) and the stomach are intraperitoneal and anterior to the superior mesenteric artery

literature, albeit briefly [28]. Recently, this rationale has been applied for excluding malrotation by US [35] but without any reference to the feasibility and the success rate of the technique.

This study was performed to assess the feasibility and the success rate of a bedside US study in demonstrating the D3 between the SMA and the aorta in an attempt to exclude malrotation and potentially obviate the need for UGI.

Material and methods

Thirty-three infants were scanned by a pediatric radiologist with 26 years' experience in pediatric US. All infants were born after IRB approval of the protocol and were 1 day to 2 days old at the time of the US study. The US studies were performed at bedside in the full-term nursery (30 infants) and neonatal intensive care unit (NICU, three infants). Vital signs of the NICU patients were continuously monitored. In obtaining consent, the parent was informed that if the US study could not demonstrate a normal retromesenteric D3, then the child would undergo a UGI for further evaluation. UGI evaluations were not performed in cases in which US showed a normal retromesenteric D3.

US technique

Imaging was performed on a Philips iU22 system (Bothell, WA, USA) using a high resolution and small footprint curvilinear (C8-5) and linear (L9-3) transducers. The acoustic window was the anterior abdominal wall. No attempt was made to lessen the bowel gas or better outline the D3 by offering oral intake. No sedation or US contrast agents were used. Gentle graded compression was applied as needed. The physical force of the compression applied was comparable to that applied in palpating an infant's abdominal organs during a routine physical examination. Serial axial and sagittal images were obtained looking for the following anatomic landmarks in sequence.

Axial plane

- The confluence of splenic vein with the superior mesenteric vein (SMV), with the pancreas always in the image
- At a slightly lower level, the left renal vein crossing from left to right between the SMA and the aorta and draining into the inferior vena cava (IVC)
- Slightly lower, in case of leftward jejunum, the first left jejunal vein
- At the same or slightly lower level, D3 anterior and inferior to the renal and posterior to the jejunal veins and adjacent to the uncinate process

Table 1 Characteristics of the third portion of the duodenum (D3) in 33 neonates

Visible retromesenteric D3	33
D3 passes midline to the left side	33
D3 appearance:	
Homogeneous tissue	10
Mucosa & muscularis	4
Fluid-filled	4
Containing air	11
Containing air & fluid	4
D3 anteroposterior dimension	range: 2–9 mm (mean: 6 mm)
D3 cephalocaudad dimension	range: 18–28 mm (mean: 22 mm)

Longitudinal plane

- D3 between the SMA and SMV and the abdominal aorta and anterior to the renal vein

While US was being performed, the routine vital signs of the infants were monitored by their nurses. Recording the length of the exam was assisted by using the time shown on the equipment's monitor, from the starting point to completion of recording of relevant images. This included time to change transducers. The length of time from transducer placement to satisfactory visualization of the retromesenteric D3 in the axial plane was recorded.

For comparison, a case of surgically proven, uncomplicated malrotation was also studied.

Results

The female/male ratio of the infants was 20/13, including 25 African Americans, five Caucasians, two Hispanics, and one Asian. The birth weight ranged from 1,265 g to 4,265 g, with mean of 3,004 g.

The small footprint C8-5 curvilinear transducer, commonly used for neonatal head and abdominal US, was used in 32 infants for axial and in 29 for longitudinal imaging. The C8-5 transducer was used alone in 11 infants. The L9-3 transducer was also used in 21 infants for axial imaging and in 14 for longitudinal imaging.

The characteristics of retromesenteric D3 in 33 babies are tabulated (Table 1). Three other anatomic structures were also noted between the SMA/SMV and the aorta. These included the uncinate process of the pancreas, the left renal vein, and jejunal veins. The most medial aspect of the uncinate process of the pancreas had the same echogenicity as the rest of the pancreas and different echogenicity from D3 (Fig. 3). The uncinate process approached but never crossed the midline to the left of the spine. The left renal vein was immediately anterior to the aorta and posterosuperior to the retromesenteric D3 (Fig. 4). The jejunal veins were mostly behind the superior mesenteric vessels and anterior to D3 and the aorta (Fig. 4). Less often, the first jejunal vein was anterior to the SMA (Fig. 5).

D3 was either homogeneous or mildly hypoechoic or with mildly echogenic mucosa and hypoechoic muscularis (Fig. 5), extending beyond the midline toward the left (Fig. 6). It often contained gas, fluid or both (Fig. 7). The anterior/posterior dimension of the D3 in the transverse plane was invariably smaller than that in the longitudinal plane (Fig. 8).

In the longitudinal plane, D3 bowed the SMA and SMV anteriorly with a cephalocaudad dimension of up to 28 mm (Figs. 4 and 8). This stood out in sharp contrast with the comparison patient, who had malrotation without volvulus, where the SMA was very close and parallel to the aorta with no retromesenteric D3 in between (Fig. 9).

Substantial bowel gas was present in 15 infants (45.4%), obscuring the three essential anatomic structures, the aorta, the SMA/SMV and the D3 in between. After applying graded compression, first a narrow window opened through which the three essential anatomic structures were successfully displayed. With sustained compression, the window widened, yielding greater information (Fig. 10). This task was accomplished also by using the linear transducer, but less

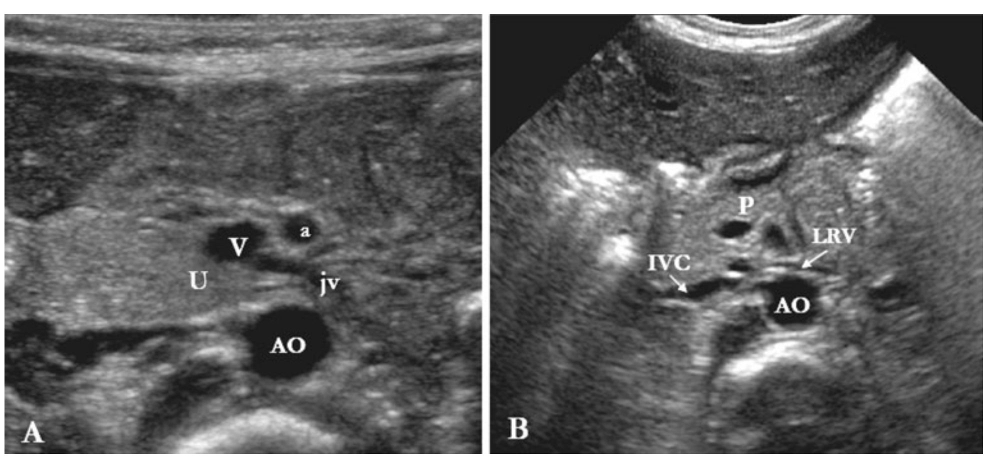

Fig. 3 US imaging of a 1-day-old girl. **a** Axial image represents the uncinate process (*U*), SMV, SMA (*V* and *a*), the jejunal vein (*jv*) and the aorta (*AO*). **b** Note that the echogenicity of the uncinate process (*U*) in (**a**) is identical to that of the body of the pancreas (*P*) in (**b**). The retromesenteric left renal vein (*LRV*) is draining to the IVC

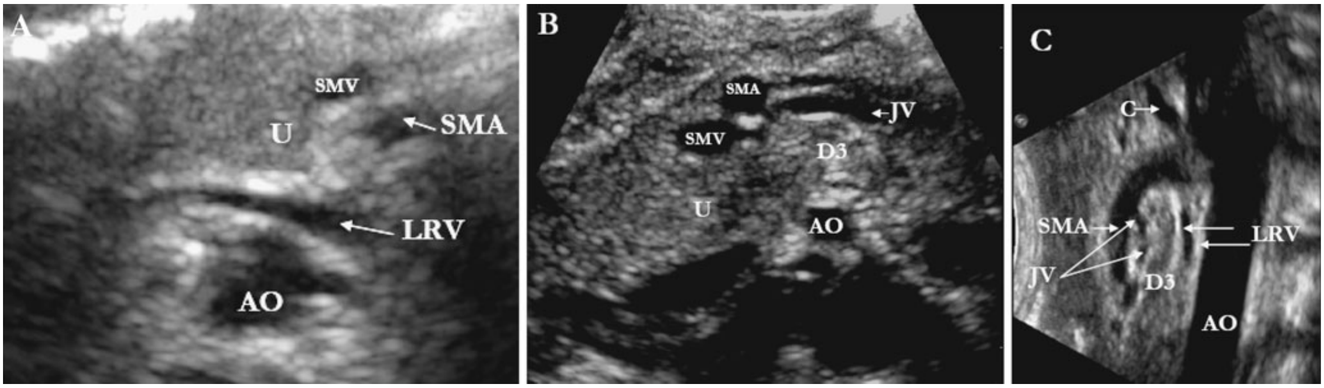

Fig. 4 US imaging of a 1-day-old girl. **a** The left renal vein (*LRV*) runs from left to right between the aorta (*AO*) and the superior mesenteric artery (*SMA*) and vein (*SMV*), with the uncinate process (*U*) also visible. **b** Axial sonogram demonstrates the retromesenteric jejunal vein (*JV*) draining into the SMV, the AO and the D3 in between the AO and SMA/SMV. **c** Vertically oriented longitudinal image shows the jejunal veins (*long arrows*) behind the SMA and anterior to the D3, and the left renal vein (*LRV*) anterior to the aorta (*AO*) and posterior to the D3. C represents the celiac axis. Note that the SMA is bowed anteriorly by the D3

successfully because of a much larger footprint, therefore, a less effective compression force.

The SMA and SMV were side by side in 31 infants and anteroposterior in 2 (Table 2) (Fig. 7). They were situated in midline anterior to the aorta in 15 infants (Figs. 3, 8, and 10), to the right of the aorta in 9 (Figs. 6 and 7), to the left of the aorta in 3 (Fig. 5), and shifted during the examination in 6 infants. The SMA had an oblique course in the transverse plane, heading toward ten o'clock in two babies, causing the so-called SMA cut-off sign in the longitudinal plane. After gentle compression on the right side, the SMA cut-off sign resolved as the SMA aligned with the aorta with D3 in between, anterior to the left renal vein (Fig. 11). In nine infants, the SMA was not surrounded by fat.

It took an average of 34 s (range 6 s to 5 min 17 s) to display the retromesenteric D3 in the axial plane. The average time for doing the entire study, including documenting the starting point, printing the relevant images and changing the transducers, was 2 min 58 s.

No changes in vital signs were observed in any of the three NICU patients during the US examination.

Discussion

The UGI criteria for diagnosis or exclusion of malrotation in frontal and lateral projections have been well described and are based on the position of the duodenojejunal

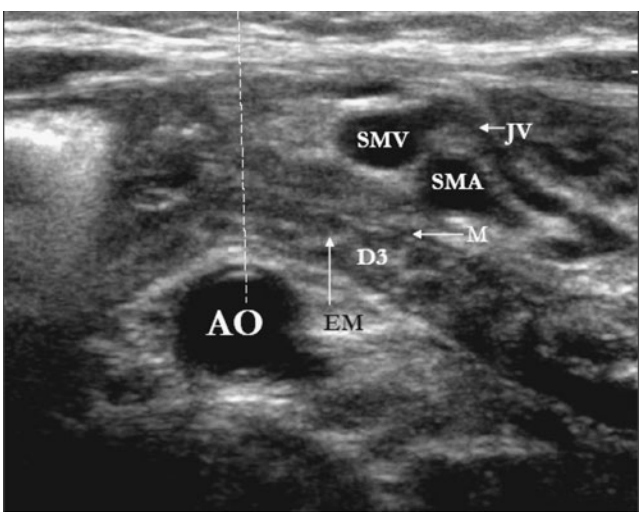

Fig. 5 US imaging of a 2-day-old girl. Axial images demonstrate the jejunal vein (*JV*) emptying into the SMV anterior to the SMA. The D3 is well seen between the AO and the SMA/SMV with echogenic mucosa (*EM*) and hypoechoic muscularis (*M*). The SMA and SMV are quite to the left of the *dashed line* through the mid-aorta

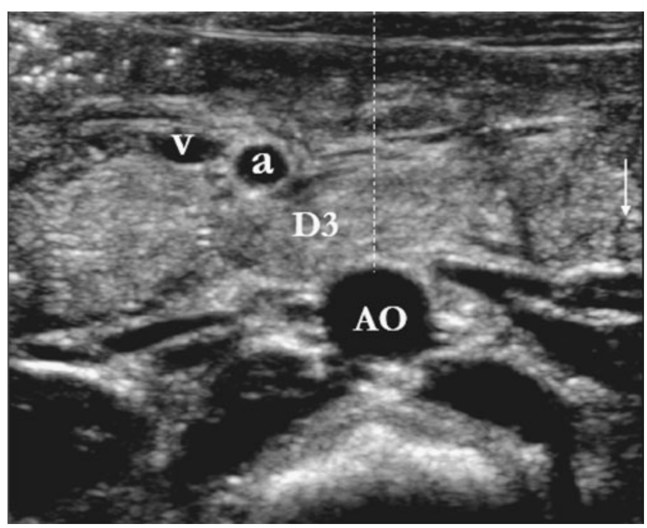

Fig. 6 US imaging of a 1-day-old girl. Axial sonogram shows the homogeneous D3 extending way to the left of the dashed mid-aortic line to the left margin of the image (*arrow*) and the SMA/SMV (*a* and *v*) to the right of the dashed mid-aortic line

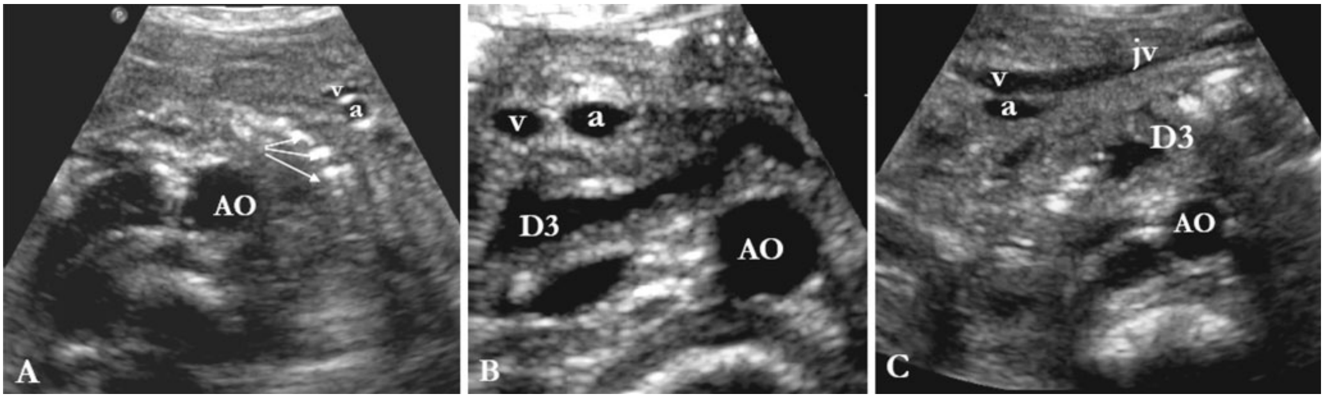

Fig. 7 US imaging. **a** Axial images demonstrate the D3 between the AO and the SMA/SMV containing only gas (*arrows*). **b** The D3 contains only fluid. **c** The D3 contains gas and fluid combined. Aorta (*AO*), SMA/SMV (*a* and *v*), and the 3rd portion of the duodenum (D3) are annotated. Note the SMV (*v*) is anterior to the SMV (*a*) and the left jejunal vein (*jv*) is anterior to the SMA

junction [29]. Accordingly, if these criteria are not met, then the diagnosis of malrotation is entertained [29]. However, despite even technically perfect examinations, 100% accurate diagnosis/exclusion of malrotation might not be achieved [30] because the duodenojejunal junction can be displaced either inferiorly, medially or both, mimicking malrotation. Such displacement can occur as a result of splenomegaly, liver transplant [8], gastric and small bowel distention [4], and rightward jejunum [35].

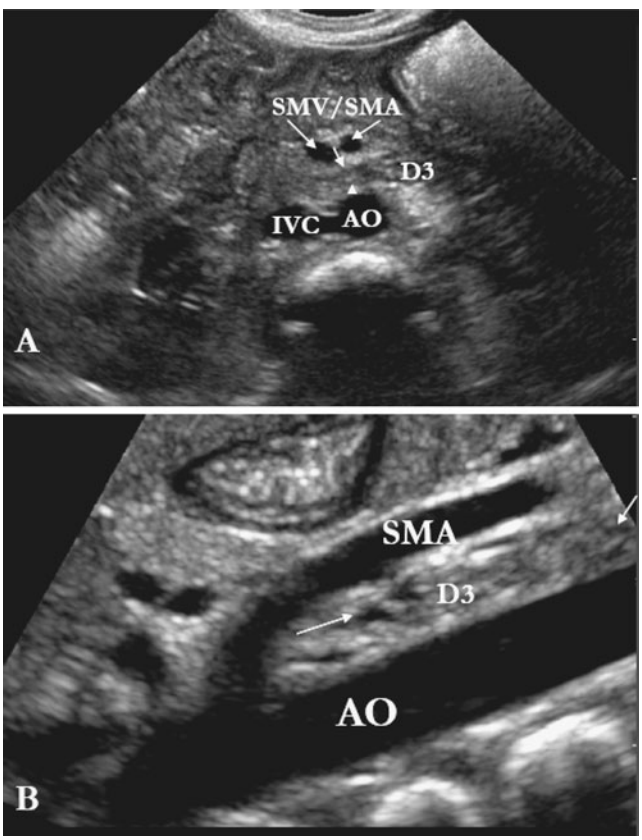

Fig. 8 US imaging of a 1-day-old girl. **a** Axial plane, narrow AP dimension of the D3 is between the *three small arrows* and the *arrowhead*. **b** Longitudinal plane, longer D3 in cephalocaudad dimension (between *arrows*). The AO, the IVC, the SMA and the SMV are noted

Recently, the relaxation of the fibromuscular ligament of Treitz has been implicated as a cause of false-positive UGI [40, 41]. Novel and intriguing as this anatomic and physiologic reminder might be, at best it only serves as an afterthought for explaining the cause of a false-positive interpretation without preventing the same error in a subsequent case. Last, it has been suggested that in equivocal cases in which repeated imaging has failed, surgical exploration using laparoscopy might be considered [31].

We believe that the US illustration of the retromesenteric D3 is feasible and has the potential to exclude malrotation for the following reasons:

(1) Normally, D3 is situated in the retroperitoneal compartment between the SMA and aorta. In malrotation, D3 is always intraperitoneal and anterior to the SMA.
(2) A retromesenteric D3 indicates that the gut has reached its final embryologic destination, fixed in the retroperitoneal compartment, excluding malrotation.
(3) Neither does the "normal" position of the duodenojejunal junction prove the existence of the ligament of Treitz, nor does its "abnormal" position prove the absence of the ligament of Treitz. One can only infer the existence of the ligament of Treitz by demonstrating the retromesenteric D3. However, confirmation of the retromesenteric location of D3 renders the existence of the ligament of Treitz a moot point.
(4) Many factors can cause displacement of the duodenojejunal junction but none should alter the retromesenteric location of D3 [35].

In this study, we successfully illustrated the retromesenteric D3 in 100% of 33 newborns. This occurred despite the

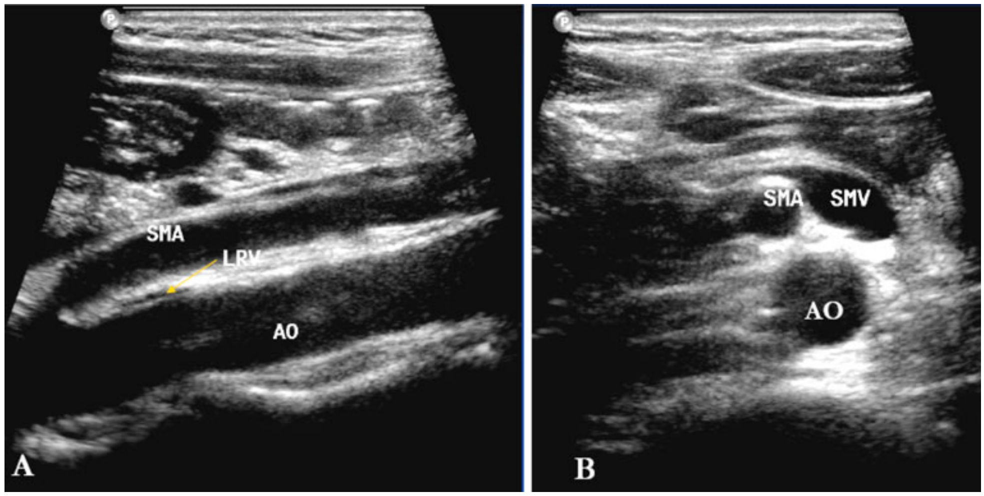

Fig. 9 US imaging of 10-year-old girl with surgically proven malrotation. **a** The SMA is parallel and very near to the AO with no D3 in between in a girl with malrotation. The left renal vein is shown (*arrow*). **b** Reversed orientation of the mesenteric vessels. No D3 is seen between the SMA/SMV and the AO

gas-filled bowel loops encountered in 45% of the infants. Bowel gas poses a challenge and can cause the operator to abort the study. However, with the aid of graded compression, the acoustic window is opened and the essential anatomic elements, the aorta, the SMA and SMV, and the retromesenteric D3 can be adequately seen.

The ease and practicality of the method is proved by the average 34-sec duration for demonstration of the retromesenteric D3 in the axial plane. As with all US studies, this one can be performed portably, avoiding the need to transport the infant to the radiology department.

Aside from the D3, three neighboring anatomic structures are normally seen between the aorta and the proximal SMA. These include the left renal vein, the jejunal veins and the uncinate process of the pancreas. Among all bowel loops, only D3 is a normal retromesenteric, retroperitoneal structure. The jejunum and the transverse colon are both intraperitoneal and anterior to the SMA. Features that characterize D3 are: (1) location anterior and inferior to the left renal vein, (2) location posterior to the jejunal veins, and (3) intimate adjacency to the uncinate process. If these nearby structures are not seen, then the plane of the imaging is inferior to where it should be. Although the isthmus of a horseshoe kidney is anterior to the aorta, it will be caudad to D3 rather than adjacent to these normal structures that are adjacent to D3.

The normally prominent uncinate process should not pose any problem in identification because its echogenicity is identical to that of the rest of the pancreas and is greater than that of the retromesenteric D3. Also, unlike the retromesenteric D3, the uncinate process does not cross the midline. Furthermore, genesis of the uncinate process is contingent to the normal development of the duodenal sweep. Absence of the uncinate process is a finding known to occur in patients with malrotation, and the display of a normally prominent uncinate process alone militates against malrotation [42].

Early CT and US literature examined the reliability of the relative positions of the superior mesenteric vessels in diagnosing or excluding malrotation [13–21]. However, further investigations proved the optimism to be unwarranted [22, 23]. In this feasibility study, the position of the SMA and SMV was variable, either to the right or to the

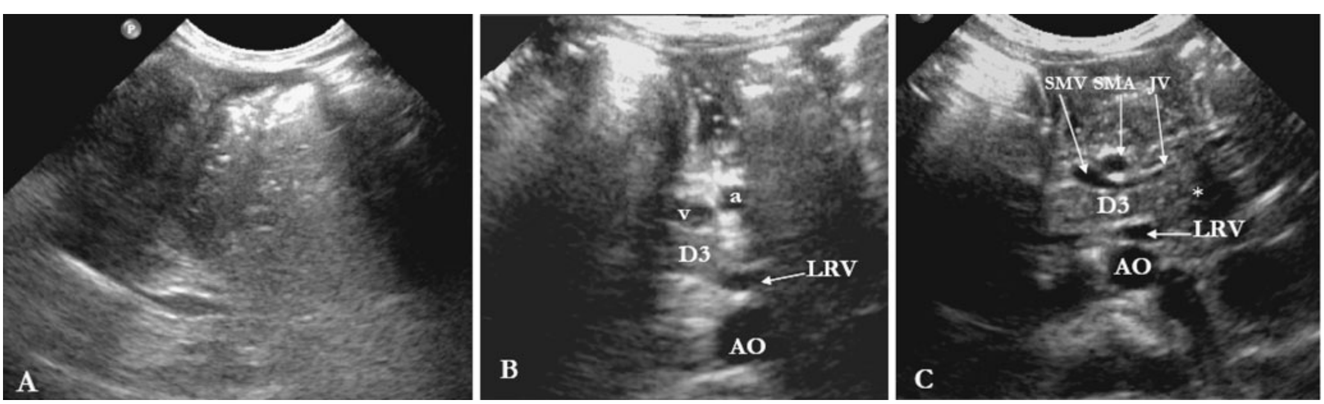

Fig. 10 US imaging of a 1-day-old boy. **a** Axial plane image demonstrates the gas block at the onset of a study before graded compression was conducted. **b** Early image after graded compression. The AO, the SMA/SMV (*a* and *v*), and the D3 in between are shown, with a part of the LRV behind the D3 anterior to the AO. **c** Later, with the visual window open wider, the left jejunal vein (*JV*) can also be seen. Note that the homogeneous D3 extends beyond the midline to the left (*)

Table 2 Characteristics of the superior mesenteric artery (SMA) and superior mesenteric vein (SMV) in 33 neonates

SMA & SMV position	
Midline, anterior to the aorta	15
To the right of the mid aorta	9
To the left of the mid aorta	3
Shifting position during the study	6
Fat around the SMA	24
SMA side by side with SMV	31
SMV anterior to the SMV	2
SMA cut off sign	3

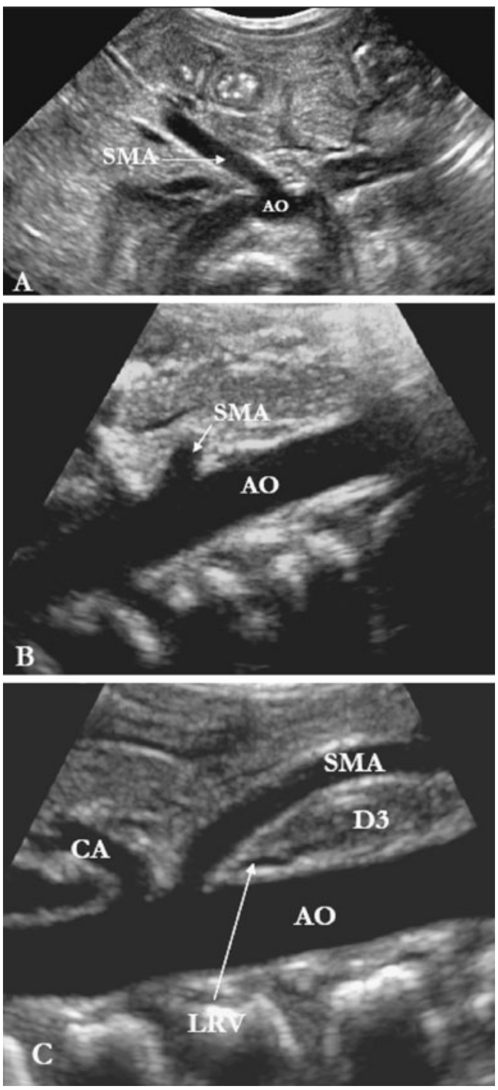

Fig. 11 US imaging of a 1-day-old girl. a Axial scan shows the SMA pointing to ten o'clock and an indistinct position of the D3. **b** Longitudinal scan shows the SMA cut-off sign. **c** After gentle compression on the right side of the abdomen, longitudinal imaging shows the SMA aligned with the AO and the D3 in between and anterior to the left renal artery (*LRV*). Note the celiac artery (*CA*)

left of the midline or shifting during the examination in 18/33 (nearly 55%) neonates. With SMV anterior to the SMA in two neonates and the so-called SMA cut-off sign in three others, the potential for US false-positives was encountered in five of 33 infants (15%), supporting prior studies that the relative position of the superior mesenteric vessels in diagnosing or excluding the malrotation is not trustworthy [22, 23]. With mild compression on the right side of the abdomen, the cut-off sign resolved in our cases and the SMA aligned with the aorta, with D3 in between.

Rightward shift of the SMA and SMV seen in nine infants was caused by the rightward shift of the proximal jejunum. This was corrected by gentle compression on the right side of the abdomen and shifting the jejunum back to the left and SMA and SMV to the midline. With this maneuver, the retromesenteric D3 could be shown between SMA and the aorta in the longitudinal plane.

Limitations

This feasibility study addressed the practicality of the US technique only in newborns. Although malrotation and malrotation with volvulus most commonly present in the neonatal period, our patient population does not match the population presenting clinically for evaluation of suspected malrotation or malrotation with volvulus. Additional study is required to verify that the described technique is feasible in a broader patient population, particularly older children.

US scanning was performed by a single pediatric radiologist with 26 years of experience in US. US examination is operator-dependent and the success of this technique will rely very heavily on the experience, skills and diligence of the individuals performing the US scanning. As with US in the diagnosis of pyloric stenosis, there will be a learning curve for training of US technologists. At our institution, all four US technologists have achieved competence to do the study well without supervision. Additional study is required to demonstrate that the techniques described can be performed with high accuracy by other investigators, particularly those with less experience, and at other institutions.

We did not attempt to sonographically follow the course of the duodenum from stomach to D3. This technique might improve identification of D3; however, the feasibility of this maneuver is unknown. However, no other bowel loop is situated in the retromesenteric space. Therefore, demonstration of continuity with proximal duodenum and stomach is not necessary.

Most important, this is a study of feasibility. The gold standard in this study is normal anatomic expectations and embryologic principles. The US findings were not proved by comparison to surgery or other cross-sectional imaging because the IRB approval would not have been possible.

Conclusion

We have studied a simple and intuitively logical US technique that is based on fundamentals of normal embryology and anatomy. As with surgical visualization, US identification of the retromesenteric D3 indicates that the gut has completed its embryologic journey and is secured in the retroperitoneal compartment. We have shown that it is feasible to identify the retromesenteric D3 with US in newborns. Further studies using a broader patient population and in comparison to surgical findings and other cross-sectional imaging studies might be required to validate our technique and its clinical utility. US of the retromesenteric third portion of the duodenum provides confirmation of normal duodenal anatomy. This technique, therefore, bears great promise for excluding malrotation without the need for ionizing radiation.

Acknowledgements The authors wish to thank Dr. David Paushter for his encouragement and support; Dr. William Meadow, neonatologist, for authorizing our study; Dr. Mario Zaritzky for his expertise as a former pediatric surgeon and his computer assistance, and Pennie Stivan for facilitating technologists' participation. We also thank Sheila A. Mitchell for her secretarial assistance.

References

1. Rescorla FJ, Shedd FJ, Grosfeld JL et al (1990) Anomalies of intestinal rotation in childhood: analysis of 447 cases. Surgery 108:710–715
2. Dilley AV, Pereira J, Shi EC et al (2000) The radiologist says malrotation: does the surgeon operate? Pediatr Surg Int 16:45–49
3. Berdon WE, Baker DH, Bull S et al (1970) Midgut malrotation and volvulus. Radiology 96:375–383
4. Applegate KE, Anderson JM, Klatte EC (2006) Intestinal malrotation in children: a problem-solving approach to the upper gastrointestinal series. Radiographics 26:1485–1500
5. Long FR, Kramer SS, Markowitz RI et al (1996) Intestinal malrotation in children: tutorial on radiographic diagnosis in difficult cases. Radiology 198:775–780
6. Strouse PJ (2004) Disorders of intestinal rotation and fixation ('malrotation'). Pediatr Radiol 34:837–851
7. Blachar A, Federle MP, Brancatelli G et al (2001) Radiologist performance in the diagnosis of internal hernia by using specific CT findings with emphasis on transmesenteric hernia. Radiology 221:422
8. Benya EC, Ben-Ami TE, Whitington PF et al (1998) Duodenum and duodenal-jejunal junction in children: position and appearance after liver transplantation. Radiology 207:233–236
9. Katz ME, Siegel MJ, Shackelford GD et al (1987) The position and mobility of the duodenum in children. AJR 148:947–951
10. Yousefzadeh DK, Soper RT, Jackson JH (1980) Diagnostic advantages of manual compression fluoroscopy in the radiologic work-up of vomiting neonates. J Pediatr Surg 15:270–278
11. Lim-Dunham JE, Ben-Ami TE, Yousefzadeh DK (1999) Manual epigastric compression during upper gastrointestinal examination of neonates: value in diagnosis of intestinal malrotation and volvulus. AJR 173:979–983
12. Millar AJ, Rode H, Brown RA et al (1987) The deadly vomit: malrotation and midget volvulus. A review of 137 cases. Pediatr Surg Int 2:172–174
13. Loyer E, Eggli KD (1989) Sonographic evaluation of superior mesenteric vascular relationship in malrotation. Pediatr Radiol 19:173–175
14. Dufour D, Delaet MH, Dassonville M et al (1992) Midgut malrotation, the reliability of sonographic diagnosis. Pediatr Radiol 22:21–23
15. Orzech N, Navarro OM, Langer JC (2006) Is ultrasonography a good screening test for intestinal malrotation. J Pediatr Surg 41:1005–1009
16. Sze RW, Guillerman P, Krauter D et al (2002) Case reports. A possible new ancillary sign for diagnosing midgut volvulus: the truncated superior mesenteric artery. J Ultrasound Med 21:477–480
17. Patino MO, Munden MM (2004) Utility of the sonographic whirlpool sign in diagnosing midgut volvulus in patients with atypical clinical presentations. J Ultrasound Med 23:397–401
18. Shimanuki Y, Aihara T, Takano H et al (1996) Clockwise whirlpool sign at color Doppler US: an objective and definite sign of midgut volvulus. Radiology 199:261–264
19. Pracros JP, Sann L, Genin G et al (1992) Ultrasound diagnosis of midgut volvulus: the "whirlpool" sign. Pediatr Radiol 22:18–20
20. Yeh WC, Wang HP, Chen C et al (1999) Preoperative sonographic diagnosis of midgut malrotation with volvulus in adults: the "whirlpool" sign. J Clinical US 27:279–283
21. Hsu CY, Chiba Y, Fukui O et al (2004) Counterclockwise barber-pole sign on prenatal three-dimensional power Doppler sonography in a case of duodenal obstruction without intestinal malrotation. J Clinical US 32:86–90
22. Paul C, Lynne R (2005) Counterclockwise barber-pole sign on CT: SMA/SMV variance without midgut malrotation. Pediatr Radiol 35:1125–1127
23. Ashley LM, Allen S, Teele RL (2001) A normal sonogram does not exclude malrotation. Pediatr Radiol 31:354–356
24. Aidlen J, Anupindi SA, Jaramillo D et al (2005) Malrotation with midgut volvulus: CT findings of bowel infarction. Pediatr Radiol 35:529–531
25. Zissin R, Osadchy A, Gayer G et al (2002) Pictorial review CT of duodenal pathology. Br J Radiol 75:78–84
26. Zissin R, Rathaus V, Oscadchy A et al (1999) Intestinal malrotation as an incidental finding on CT in adults. Abdom Imaging 24:550–555
27. Boudiaf M, Soyer P, Terem C et al (2001) CT evaluation of small bowel obstruction. RadioGraphics 21:613–624
28. Jayaraman MV, Mayo-Smith WW, Movson S et al (2001) CT of the duodenum: an overlooked segment gets its due. Radiographics 21:S147–S160
29. Applegate KE (2009) Evidence-based diagnosis of malrotation and volvulus. Pediatr Radiol 39(Suppl 2):S161–S163
30. Daneman A (2009) Malrotation: the balance of evidence. Pediatr Radiol 39(Suppl 2):S164–S166
31. Slovis TL, Strouse PJ (2009) Malrotation: some answers but more questions. Pediatr Radiol 39:315–316
32. Han MC, Kim CW (1989) Sectional human anatomy: transverse, sagittal and coronal sections correlated with computed tomography and magnetic resonance imaging, 2nd edn. Igaku-Shoin Medical Pub, Seoul, p 120
33. Netter FH (1989) Abdominal wall in visceral midsagittal section. In: Colacino S (ed) Atlas of human anatomy. CIBA-GEIGY Corp, New Jersey, plate 333
34. Floch MN (2005) Congenital abnormalities of the small intestine. In: Floch MH, Floch NR, Kowdley KV (eds) Netter's gastroenterology. ICON Learning Systems, Carlstadt

35. Yousefzadeh DK (2009) The position of the duodenojejunal junction: the wrong horse to bet on in diagnosing or excluding malrotation. Pediatr Radiol 39(Suppl 2):S172–S177
36. Santer R, Young C, Rossi T et al (1991) Computed tomography in superior mesenteric artery syndrome. Pediatr Radiol 21:154–155
37. Hines JR, Gore RM, Ballantyne GH (1984) Superior mesenteric artery syndrome. Diagnostic criteria and therapeutic approaches. Am J Surg 148:630–632
38. Burrington JD (1976) Superior mesenteric artery syndrome in children. Am J Dis Child 130:1367–1370
39. Burrington JD, Wayne ER (1974) Obstruction of the duodenum by the superior mesenteric artery—does it exist in children? J Pediatr Surg 9:733–741
40. Lampl B, Levin TL, Berdon W et al (2009) Malrotation and midgut volvulus: a historical review and current controversies in diagnosis and management. Pediatr Radiol 39:359–366
41. Borley NR, Healy JC (2008) Abdomen and pelvis. Section 8. In: Stranding S (ed) Gray's anatomy, 40th edn. Elsevier, London, p 1127
42. Inoue Y, Nakamura H (1997) Aplasia or hypoplasia of the pancreatic uncinate process: comparison in patients with and patients without intestinal nonrotation. Radiology 205:531–533